

Search for local CP violation in $D^0 \rightarrow \pi^+ \pi^- \pi^0$ decays with the amplitude analysis

Lanxing Li^a, Evelina Gersabeck^b, Chris Parkes^a,
Elisabeth Maria Niel^c, David Friday^a,

^aThe University of Manchester

^bUniversity of Freiburg

^cCERN

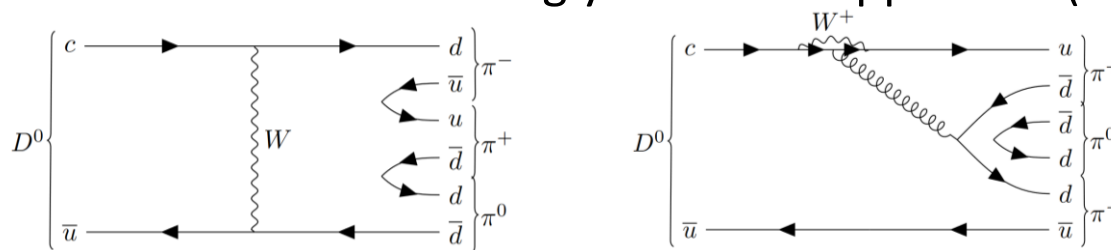
09, Apr

IOP Joint APP and HEPP Annual Conference 2025

Motivation

CP violation (CPV) is only recently discovered in charm sector via $D^0 \rightarrow h^+ h^-$ channels.

- First observation in 2019 [[Phys. Rev. Lett. 122 \(2019\) 211803](#)]:
 - $\Delta A_{\text{cp}} = A_{\text{cp}}(\text{K}^+ \text{K}^-) - A_{\text{cp}}(\pi^+ \pi^-) = (-15.4 \pm 2.9) \times 10^{-4}$
- The separated measurement in 2023 [[Phys. Rev. Lett. 131 \(2023\) 091802](#)]:
 - $A_{\text{cp}}(\text{K}^+ \text{K}^-) = (7.7 \pm 5.7) \times 10^{-4}$
 - $A_{\text{cp}}(\pi^+ \pi^-) = (-23.2 \pm 6.1) \times 10^{-4}$
- No CPV in charm multibody decays is observed yet
- $D^0 \rightarrow \pi^+ \pi^- \pi^0$ is a promising channel for CPV detection
 - Higher sensitivity possible by searching for local CPV in multibody decays
 - Large interference contributions as the strong phase varies across the phase space (PHSP)
 - Main contribution is due to Singly Cabibbo suppressed (SCS) decay



State of art: LHCb results

At the LHCb collaboration, multiple searches for CPV are performed on this channel:

- Model-independent: Energy Test (E-T) method
 - Using the LHCb Run-1 (2012) data ($\mathcal{L}_{int} = 2 \text{ fb}^{-1}$) with a signal yield $\sim 570\text{k}$ [[Phys. Lett. B 740 \(2015\) 158](#)]
 - $p = 2.6\%$
 - Using the LHCb Run-2 (2015 to 2018) data ($\mathcal{L}_{int} = 6 \text{ fb}^{-1}$) with a signal yield $\sim 2479\text{k}$ [[JHEP 09 \(2023\) 129](#)]
 - $p = 62\%$
- Time-dependent: ΔY measurement
 - Using the LHCb Run-2 (2015 to 2018) and Run-1 (2012) data ($\mathcal{L}_{int} = 7.7 \text{ fb}^{-1}$) [[Phys. Rev. Lett. 133, 101803](#)]

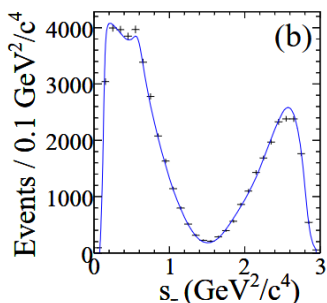
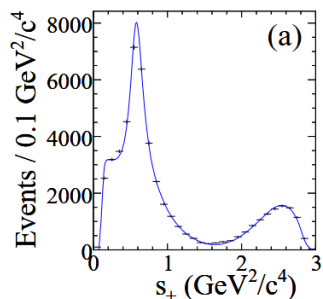
$$\Delta Y = (-1.3 \pm 6.3 \pm 2.4) \times 10^{-4}$$

While no evidence of CPV in this channel, a full amplitude analysis would be necessary, especially for future analysis, to determine any possible source of CPV.

State of art: BaBar results

The BaBar collaboration has already performed a time-integrated search for CPV via an amplitude analysis based on a 44k signal sample [[Phys. Rev. Lett. 99 251801 \(2007\)](#)]

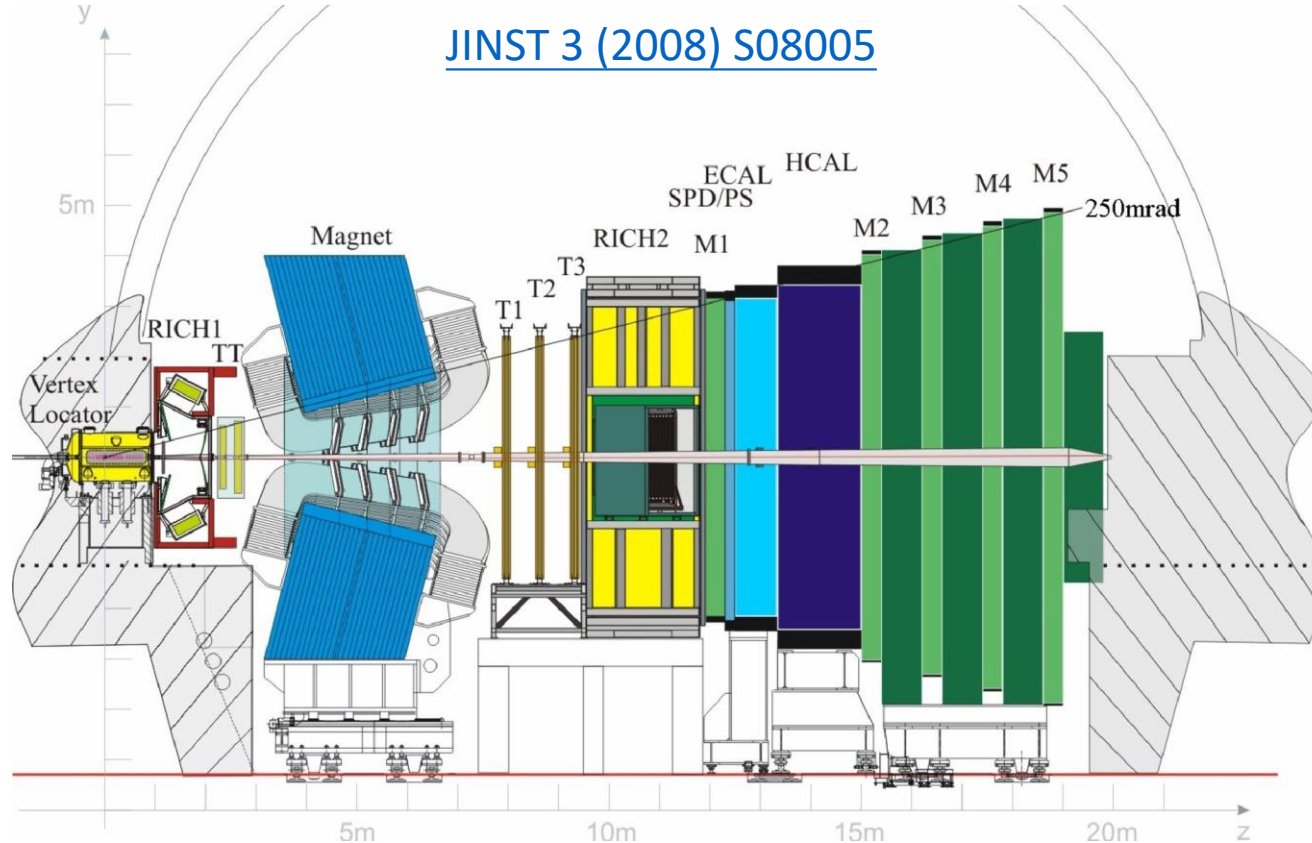
- No evidence for CPV
- S-wave parameterised by a list of f_0 resonances summed coherently.
- Sensitivity per amplitude: $\sim 1\text{-}2\%$ for the main $\rho(770)$ resonances, $\mathcal{O}(10\%)$ for others



| State | f_r (%) | Δa_r (%) | $\Delta \phi_r$ ($^\circ$) | Δf_r (%) |
|----------------|-----------|------------------------|------------------------------|------------------------|
| $\rho^+(770)$ | 68 | $-3.2 \pm 1.7 \pm 0.8$ | $-0.8 \pm 1.0 \pm 1.0$ | $-1.6 \pm 1.1 \pm 0.4$ |
| $\rho^0(770)$ | 26 | $2.1 \pm 0.9 \pm 0.5$ | $0.8 \pm 1.0 \pm 0.4$ | $1.6 \pm 1.4 \pm 0.6$ |
| $\rho^-(770)$ | 35 | $2.0 \pm 1.1 \pm 0.8$ | $-0.6 \pm 0.9 \pm 0.4$ | $0.7 \pm 1.1 \pm 0.5$ |
| $\rho^+(1450)$ | 0.1 | $2 \pm 11 \pm 8$ | $-30 \pm 25 \pm 9$ | $0.0 \pm 0.1 \pm 0.1$ |
| $\rho^0(1450)$ | 0.3 | $13 \pm 8 \pm 6$ | $-1 \pm 14 \pm 3$ | $0.1 \pm 0.2 \pm 0.1$ |
| $\rho^-(1450)$ | 1.8 | $-3 \pm 6 \pm 5$ | $8 \pm 7 \pm 3$ | $-0.2 \pm 0.3 \pm 0.1$ |
| $\rho^+(1700)$ | 4 | $19 \pm 27 \pm 9$ | $9 \pm 7 \pm 3$ | $0.4 \pm 1.0 \pm 0.4$ |
| $\rho^0(1700)$ | 5 | $-31 \pm 20 \pm 12$ | $-7 \pm 6 \pm 2$ | $-1.3 \pm 0.8 \pm 0.3$ |
| $\rho^-(1700)$ | 3 | $-3 \pm 14 \pm 11$ | $-3 \pm 8 \pm 3$ | $-0.5 \pm 0.6 \pm 0.3$ |
| $f_0(980)$ | 0.2 | $0.0 \pm 0.1 \pm 0.2$ | $-3 \pm 7 \pm 4$ | $0.0 \pm 0.1 \pm 0.1$ |
| $f_0(1370)$ | 0.4 | $-0.3 \pm 1.3 \pm 1.2$ | $7 \pm 14 \pm 5$ | $-0.2 \pm 0.1 \pm 0.1$ |
| $f_0(1500)$ | 0.4 | $0.4 \pm 1.1 \pm 0.7$ | $-1 \pm 12 \pm 1$ | $0.0 \pm 0.1 \pm 0.1$ |
| $f_0(1710)$ | 0.3 | $-3 \pm 3 \pm 2$ | $-25 \pm 13 \pm 11$ | $0.0 \pm 0.1 \pm 0.1$ |
| $f_2(1270)$ | 1.3 | $8 \pm 4 \pm 5$ | $2 \pm 5 \pm 2$ | $0.1 \pm 0.1 \pm 0.1$ |
| $\sigma(400)$ | 0.8 | $-0.3 \pm 0.7 \pm 2.0$ | $-4 \pm 7 \pm 3$ | $-0.1 \pm 0.1 \pm 0.1$ |
| Nonres | 0.8 | $12 \pm 7 \pm 8$ | $11 \pm 9 \pm 4$ | $0.2 \pm 0.3 \pm 0.2$ |

An amplitude analysis with $\sim 125\text{k}$ [[Phys. Rev. D 93 112014 \(2016\)](#)] signal events is also performed by the BaBar collaboration, though no CPV search

LHCb Detector: Run-I & Run-II



World's Largest sample of charm hadron decays:

- Run-I (2011-2012) : $\mathcal{L}_{int} = 3 \text{ fb}^{-1}$ @ $\sqrt{s} = 7\text{-}8 \text{ TeV}$
- Run-II (2015-2018) : $\mathcal{L}_{int} = 6 \text{ fb}^{-1}$ @ $\sqrt{s} = 13 \text{ TeV}$

Analysis overview

Data for $D^{*\pm} \rightarrow D^0 \pi_S^+$: 2016 – 2018 5.4 fb^{-1}

We separated the data into two samples based on the reconstruction of $\pi^0 \rightarrow \gamma\gamma$:

- **Resolved sample:** E_γ deposit in **separate** ECAL cell
- **Merged sample:** E_γ deposit in **the same** ECAL cell

Data Selection

- Trigger + Stripping line
- Offline selection
- Multivariable analysis (MVA) strategy – BDTD classifier
- Decay Tree Fitter (DTF) used

Amplitude Analysis

- Background (BKG) subtracted using sPlot technique
- Isobar model used
- Quasi model-independent method for formalism of the S-wave

CPV measurement

- Split D^0/\bar{D}^0 sample used
- CPV parameterized from
 - Magnitudes
 - Phase
 - Fit Fractions (FFs)
- Statistical sensitivity from blinded study

Signal yield and
distribution extracted

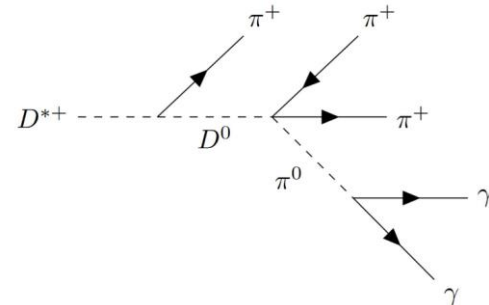
CP-averaged amplitude
model extracted

Selection overview

Most of the selection criteria are the same as the [Run-II E-T analysis](#).

Decay Tree Fitter (DTF) is used with:

- Primary vertex constraint on the D^*
- D^0/π^0 mass is constrained to the PDG value (for DP variables)



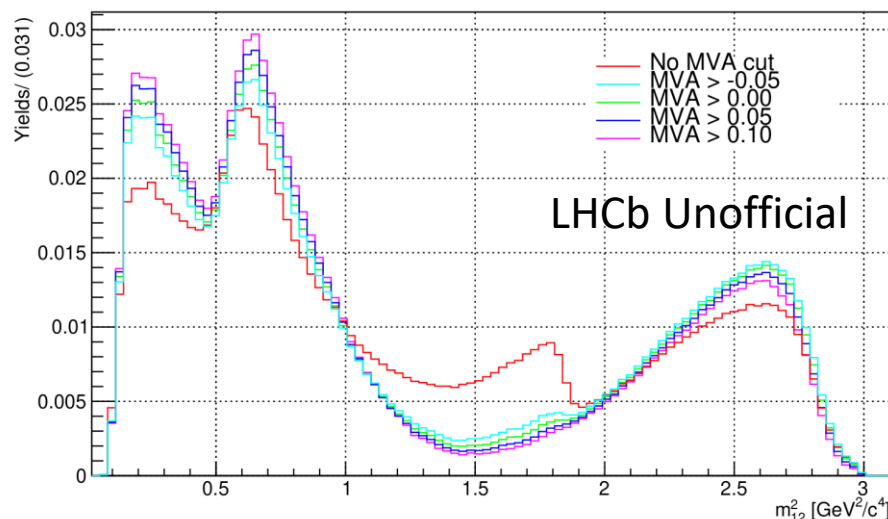
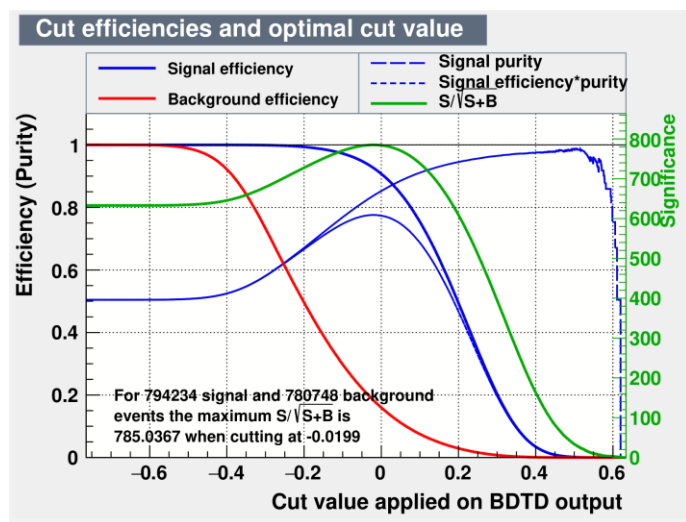
Offline selections:

- All the decay candidates are required to pass:
 - Hardware (L0) and software trigger requirements (HLT1 & HLT2)
 - A set of loose preselection processes (stripping)
- A set of customised selection criteria is then applied to improve the signal purity and suppress BKG:
 1. $|m(\pi^0 - 135)| < 28 \text{ MeV}/c^2$ (merged sample only)
 2. $|m(D^0 - 1864.84)| < 60 \text{ MeV}/c^2$
 3. Removal of cloned tracks ($\sim 1\%$ for resolved/merged sample)
 4. Multiply candidates rejection (5.9%/2.5% for resolved/merged sample)
 5. $D^0 \rightarrow K_S^0 (\rightarrow \pi^+ \pi^-) \pi^0$ decay channel veto (4% for the combined sample)
 6. mis-identification (mis-ID) BKG checked.

Data selection: MVA classifier

To suppress the combinatorial BKG, we developed a MVA classifier (2-fold) for the resolved sample

- BKG: extracted from the sideband region of Δm distribution
- Signal: LHCb simulation samples after the same selection criteria and truth-matching
- The BDT input variables exploit final state kinematics, decay topology, and vertex quality, which are mostly from [Run-II E-T analysis](#).

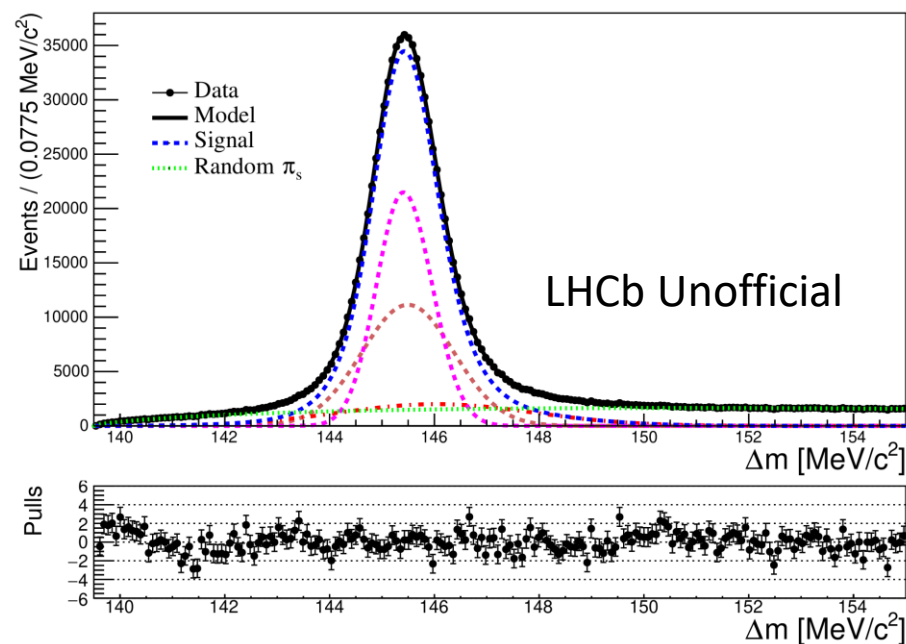
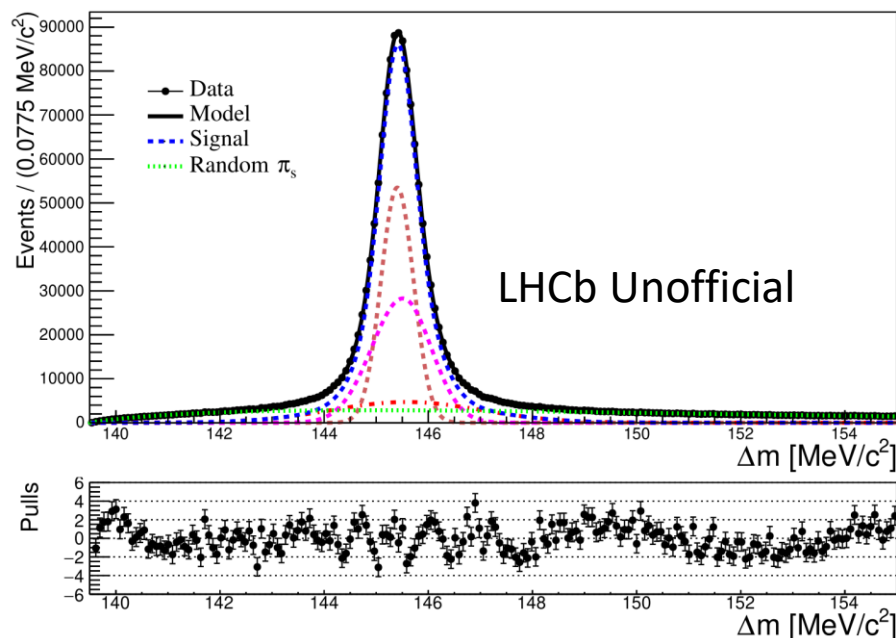


- Final cut optimised to remove the cross-feed BKG: BDTD output > 0.10

Data selection: final fitted samples

After the MVA cut, we extract the signal yield via a fit to $\Delta m = m_{D^*} - m_{D^0}$

- Signal: the sum of 2 independent Gaussian functions $(\mu_1, \mu_2 | \sigma_1, \sigma_2)$ + a bifurcated Gaussian function $(\mu_3 | \sigma_{3L}, \sigma_{3R})$
- BKG: empirical formula: $F_{bkg} = (\Delta m - m_{th})^\alpha e^{-\beta(\Delta m - m_{th})}$ ($m_{th} = 139.5 \text{ MeV}/c^2$)



| Signal($143.6 < \Delta m < 147.2 \text{ MeV}/c^2$) | Yields | Purity (%) |
|--|-----------------------------------|------------|
| Resolved | $(1010.86 \pm 2.180) \times 10^3$ | 91 |
| Merged | $(606.76 \pm 2.066) \times 10^3$ | 92 |

Amplitude fitting: model

As the decay is 3-body, Dalitz variables used to parametrise 2D phase space.

Using the Isobar model, full amplitude is written as coherent sum of components:

$$\mathcal{A}(x) = \mathcal{A}_{S\text{-Wave}} + \sum_i a^i e^{i\delta_i} \mathcal{A}_i, x = m_{ab}, M_{ac}$$

For each decays under isobar model $D \rightarrow ar(r \rightarrow bc)$, the amplitude is:

$$A_r(m_{ab}^2, m_{ac}^2) = F_D^L(q, q_0) Z_L(m_{ab}^2, m_{ac}^2) \mathcal{T}_r(m_{bc}) F_r^L(p, p_0)$$

- Here F_D^L and F_r^L are the Blatt-Weisskopf barrier factors under relative orbital angular L between r and a , Z_L is the spin factor for a resonance with spin L , and \mathcal{T}_r is the propagator describing the dynamics of the resonance decay.

Total PDF used (where the BKG is subtracted using S-weight, R_3 represents the PHSP function, ϵ is the efficiency variation across the Dalitz Plot, $S(x; c) = |A(x; c)|^2$ is the signal model based on the total amplitude $A(x)$):

$$P(x; c) = \frac{\epsilon(x) R_3(S(x; c))}{I(c)} =, I(c) = \int \epsilon(x) R_3 S(x; c) dx$$

Amplitude fitting: likelihood

After adding a relevant event-by-event S-weight, the total log-likelihood function is written

$$\begin{aligned} -2\ln\mathcal{L}_{P(x)} &= -2 \frac{\sum_i SW_i}{\sum_i SW_i^2} \sum_i SW_i \log(P(x; c)) \\ &= -2 \frac{\sum_i SW_i}{\sum_i SW_i^2} \sum_i SW_i [\log(S(x; c)) + \log(\epsilon(x)R_3) - \log(I(c))] \\ &\hspace{15em} \text{Model-independent} \end{aligned}$$

Since the efficiency and phase density do not depend on the fit parameters, the likelihood can be factorised out.

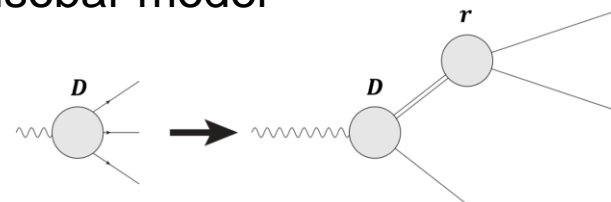
For normalisation integral $I(c)$, it can be approximated using the MC samples which are generated using a signal model $S_{\text{gen}}(x)$ and passed through all the detector reconstruction and selection procedures :

$$I(c) \approx \frac{1}{N_{mc}} \sum_{i=1}^{N_{mc}} \frac{\epsilon(x)R_3 S(x; c)}{P_{\text{gen}}(x_i)} = \frac{1}{N_{mc}} \sum_{i=1}^{N_{mc}} \frac{S(x; c)}{S_{\text{gen}}(x_i)} I_{\text{gen}}$$

In which case we avoid the explicit form of the efficiency variation across the Dalitz Plot.

Amplitude fitting: resonances

Spin 1 and spin 2 components included through the isobar model



| Resonance | Spin | Lineshape | $m(\text{MeV}/c^2)$ | $\Gamma(\text{MeV}/c^2)$ |
|------------------|------|------------------------|---------------------|--------------------------|
| $\rho(770)^0$ | 1 | $\rho - \omega$ mixing | 775.26 | 149.1 |
| $\rho(770)^\pm$ | | GS | | |
| $\omega(782)$ | 1 | $\rho - \omega$ mixing | 782.66 | 8.68 |
| $\rho(1450)^0$ | 1 | GS | 1465 | 400 |
| $\rho(1400)^\pm$ | | GS | | |
| $\rho(1700)^0$ | 1 | GS | 1720 | 250 |
| $\rho(1700)^\pm$ | | GS | | |
| $f_2(1270)$ | 2 | RBW | 1275.5 | 186.7 |

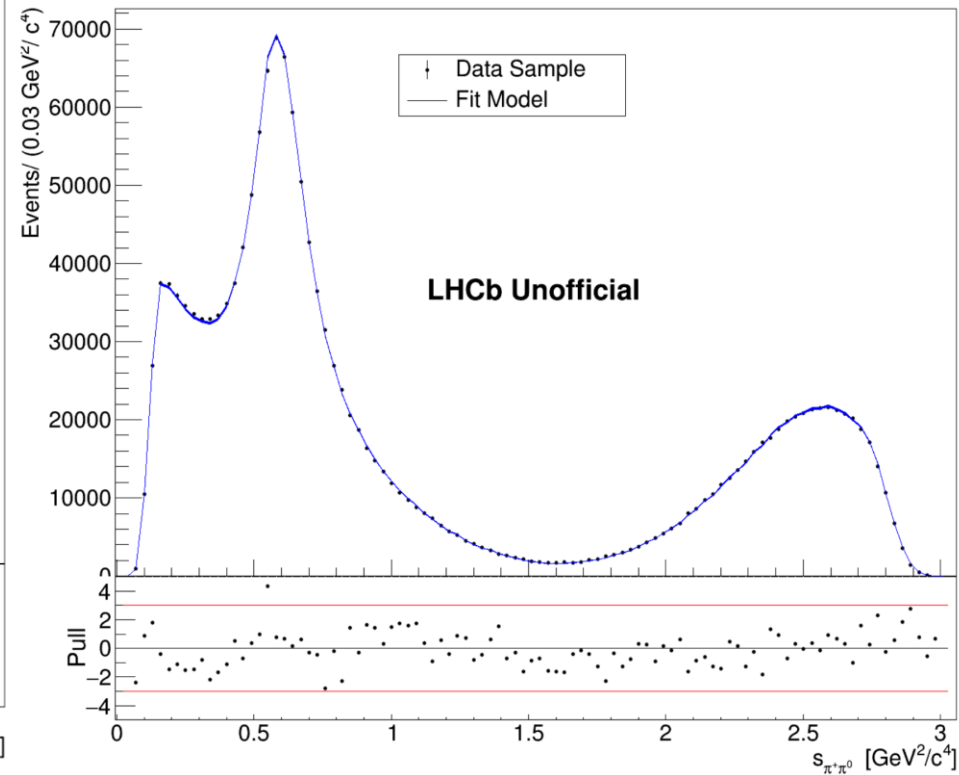
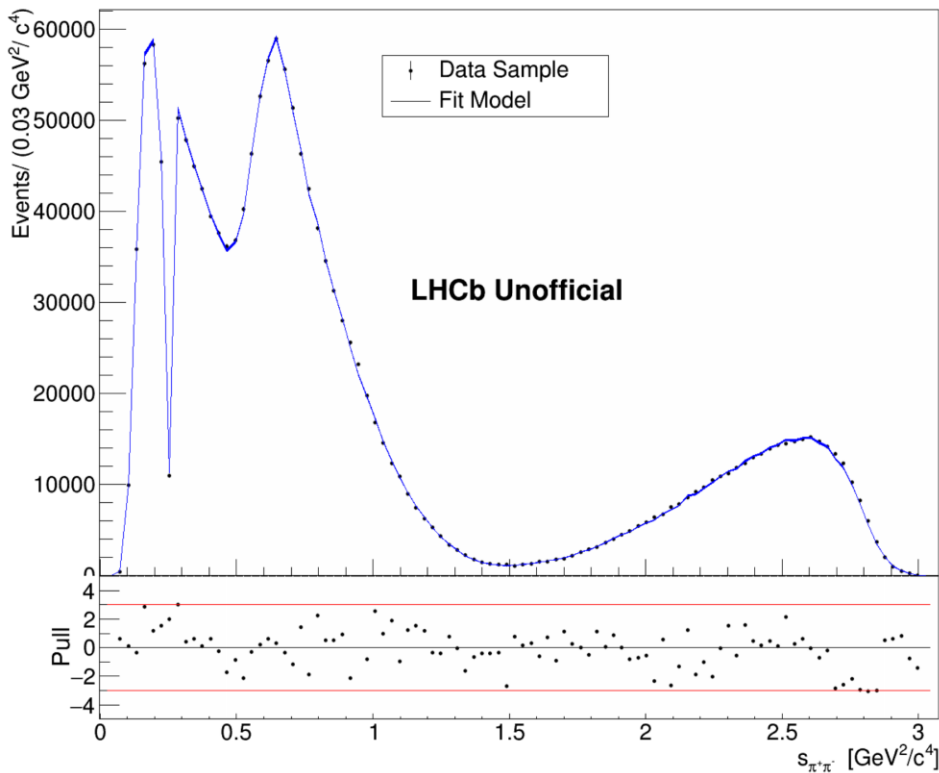
- RBW: Relativistic Breit-Wigner
- GS: Gounaris-Sakurai
- $\rho - \omega$ mixing: $\rho - \omega$ mixing lineshape [[Commun.Theor.Phys. 69 \(2018\) 1, 50](#)]

Baseline model:

- P-wave: ρ resonances, $\omega(782)$ (mass/width fixed to PDG value)
- D-wave: $f_2(1270)$
- S-wave: QMIPWA model (Quasi Model-Independent Partial Wave Analysis) [[JHEP 2306 \(2023\) 044](#)]

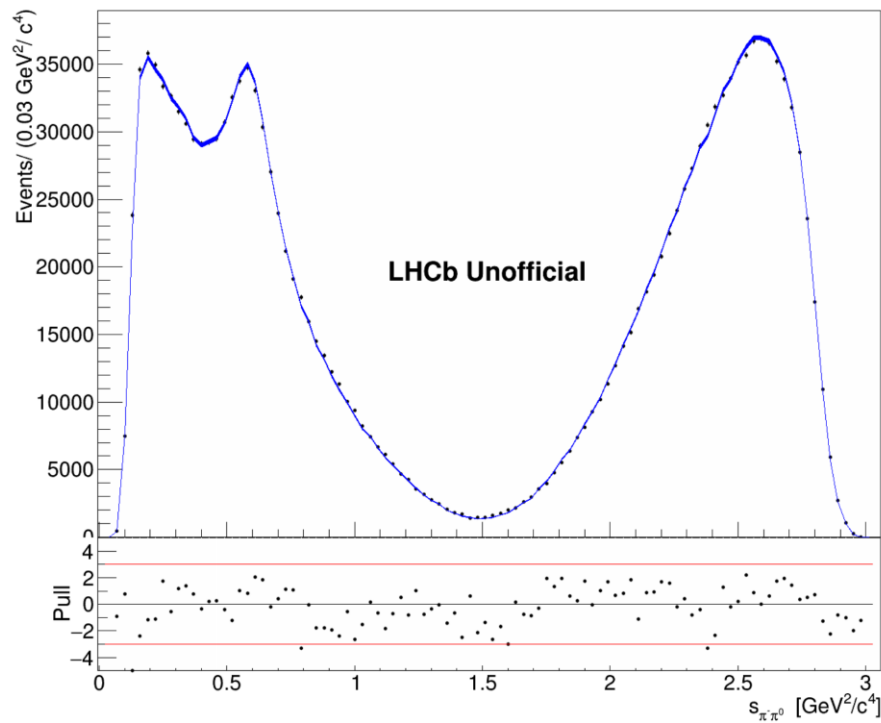
Amplitude fitting: fit result

Results of the nominal fit projected on the Dalitz variables where the QMIPWA method is used



Amplitude fitting: fit result

Results of the nominal fit projected on the Dalitz variables where the QMIPWA method is used



| System | Resonance | $ \mathcal{R}(a_r) $ | $\mathcal{I}(a_r)$ | Fit Fraction [%] |
|----------------------|----------------|----------------------|----------------------------|------------------|
| | $\rho(770)^+$ | 1.0 (fixed) | 0.0 (fixed) | 74.51 ± 0.09 |
| | $\rho(770)^0$ | 0.5919 ± 0.0008 | -2.8636 ± 0.0017 | 25.96 ± 0.07 |
| | $\rho(770)^-$ | 0.6615 ± 0.0009 | -3.1309 ± 0.0026 | 32.58 ± 0.07 |
| | $\rho(1450)^+$ | 0.0907 ± 0.0013 | 2.8929 ± 0.0169 | 0.57 ± 0.02 |
| | $\rho(1450)^0$ | 0.0482 ± 0.0014 | -1.8724 ± 0.0296 | 0.16 ± 0.01 |
| | $\rho(1450)^-$ | 0.0315 ± 0.0014 | -3.1218 ± 0.0449 | 0.07 ± 0.01 |
| | $\rho(1700)^+$ | 0.1102 ± 0.0024 | 0.2507 ± 0.0209 | 0.32 ± 0.02 |
| | $\rho(1700)^0$ | 0.1403 ± 0.0025 | 2.4972 ± 0.0197 | 0.53 ± 0.03 |
| | $\rho(1700)^-$ | 0.0996 ± 0.0021 | 2.0985 ± 0.0276 | 0.26 ± 0.01 |
| | $f_2(1270)$ | 0.1147 ± 0.0007 | 0.1271 ± 0.0012 | 0.61 ± 0.01 |
| $\pi\pi$ S-wave | 30 points | | | 2.09 ± 0.01 |
| B | | 0.0297 ± 0.002 | 3.104 ± 0.0925 | |
| δ | 4.9 MeV | | | |
| Sum of Fit Fractions | | | 137.68 ± 0.16 | |
| χ^2/ν | | | $143095.26/131033 = 1.092$ | |
| FCN | | | -3045041.2 | |

- The low FF resonances are significant in the fit when compared to the null hypothesis

Systematic uncertainties

$$\sigma_{syst}^{CP} = \sigma_{syst}^{amp} + \sigma_{syst} \text{ from other possible CPV sources}$$

- **For Amplitude Fit:**

- **Resonance description:**

- Change Gounaris-Sakurai lineshape for the neutral resonances to RBW lineshape
- Vary mass/ width of high-mass resonances within the PDG uncertainties
- Variation of the binning scheme for QMIPWA

- **Background description:**

- Change of the BKG model input to the Δm fit to extract the S-weight
- Use the COW weight as the alternative signal weight instead of S-weight

- **Efficiency variation**

- Variation of the input variables for the reweighting
- The systematic uncertainty from the finite size of the simulated sample is studied using the resampling method
- Regenerating the transformed PID variables from the resampled calibration sample with a different number of events
- L0 efficiency correction for the MC sample

- **For CPV Fit:**

- PHSP-dependent detection/production asymmetry + ...

CPV measurement: overview

Once the CP averaged D^0 model has been determined, we can use it to perform the search for CPV

- The data is split into D^0 and \bar{D}^0 samples based on the flavour of the soft pions, where CP conjugation has been applied on all \bar{D}^0 candidates
- The CPV can be parameterised using the average modulus $\overline{|a_r|}$, modulus asymmetry $A_{|a_r|}$, average phase $\overline{\arg(a_r)}$ and phase difference $\Delta \arg(a_r)$. We then calculate the CPV parameters based on the simultaneous fit result:

$$\begin{aligned}\overline{|a_r|} &= \frac{|a_r|_{D^0} + |a_r|_{\bar{D}^0}}{2}, & A_{|a_r|} &= \frac{|a_r|_{D^0} - |a_r|_{\bar{D}^0}}{|a_r|_{D^0} + |a_r|_{\bar{D}^0}} \\ \overline{\arg(a_r)} &= \frac{\arg(c)_{D^0} + \arg(c)_{\bar{D}^0}}{2}, & \Delta \arg(a_r) &= \frac{\arg(c)_{D^0} - \arg(c)_{\bar{D}^0}}{2}\end{aligned}$$

Furthermore, the fit fractions can also be used to refer to the additional CPV parameters in each amplitude:

$$A_{FF_r} = \frac{FF_{D^0} - FF_{\bar{D}^0}}{FF_{D^0} + FF_{\bar{D}^0}}$$

- **For now**, a search for the CPV is done using the blinded D^0 and \bar{D}^0 samples, where all the central value of the CPV parameters are shifted secretly.

CPV measurement: Blinded result

- Results of the CP violation from the simultaneous fit over the blinded D^0 and \bar{D}^0 samples are summarised in the table:

| Resonance | $A_{ a_r }$ ($\times 100$) | $\Delta\arg(a_r)$ ($\times 100$) | A_{FF_r} ($\times 100$) |
|-----------------|------------------------------|------------------------------------|------------------------------------|
| $\rho^+(770)$ | – | – | xx \pm 0.1316 |
| $\rho^0(770)$ | xx \pm 0.1472 | xx \pm 0.1570 | xx \pm 0.2330 |
| $\rho^-(770)$ | xx \pm 0.1392 | xx \pm 0.1799 | xx \pm 0.2562 |
| $\rho^+(1450)$ | xx \pm 2.4107 | xx \pm 2.1272 | xx \pm 4.7753 |
| $\rho^0(1450)$ | xx \pm 3.2241 | xx \pm 3.8791 | xx \pm 6.4767 |
| $\rho^-(1450)$ | xx \pm 5.5395 | xx \pm 5.1208 | xx \pm 11.0822 |
| $\rho^+(1700)$ | xx \pm 2.9153 | xx \pm 2.7706 | xx \pm 5.8381 |
| $\rho^0(1700)$ | xx \pm 2.1069 | xx \pm 2.6584 | xx \pm 4.2356 |
| $\rho^-(1700)$ | xx \pm 2.7071 | xx \pm 3.1588 | xx \pm 5.4115 |
| $f_2(1270)$ | xx \pm 0.5761 | xx \pm 2.1481 | xx \pm 1.1219 |
| $\pi\pi$ S-wave | xx \pm 0.4572 | xx \pm 0.5340 | xx \pm 0.9073 |

- The statistical uncertainties for $A_{|a_r|}$, $\Delta\arg(a_r)$ and A_{FF_r} range from 0.1% to 11%, which are correlated to the statistical uncertainties measured from the CP averaged fit result.

Conclusion

- An amplitude analysis has been performed on $D^0 \rightarrow \pi^+ \pi^- \pi^0$ decays collected during Run-II
- Higher CPV sensitivity is expected for the ρ resonances
- Analysis is under internal LHCb review, awaiting approval to unblind
- Next steps:
 - Finalise the current model and the systematic uncertainties
 - Do a CPV measurement by comparing the fit parameters from two unblinded sets of fit

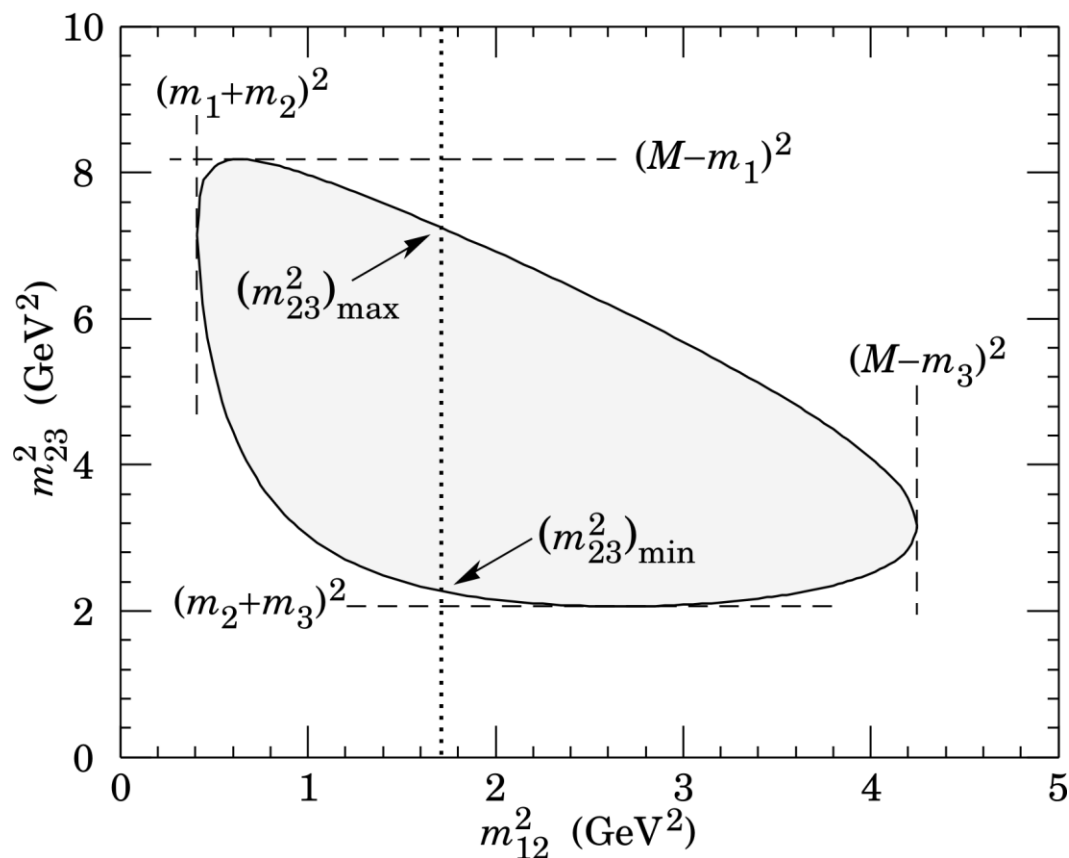


Back Up

Dalitz Plot for 2D PHSP

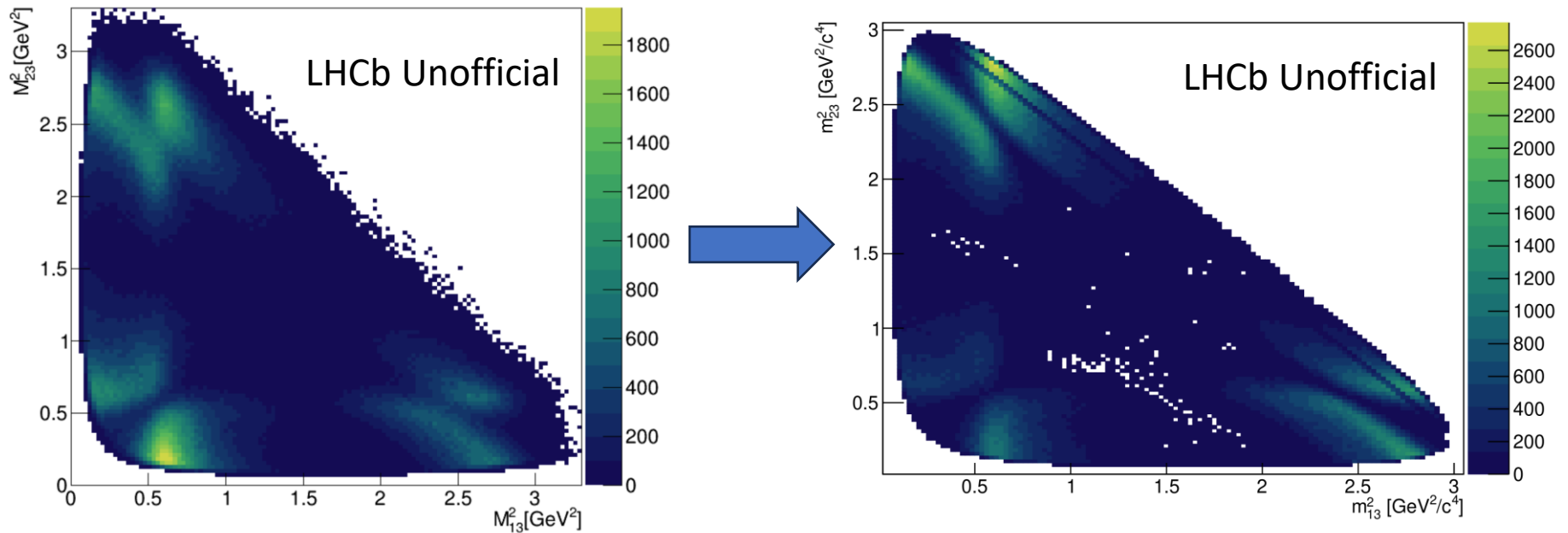
Dalitz variables used to visualise 2D phase space:

$$M_{12}: m_{\pi^+\pi^-}, M_{13}: m_{\pi^+\pi^0}, M_{23}: m_{\pi^-\pi^0}$$



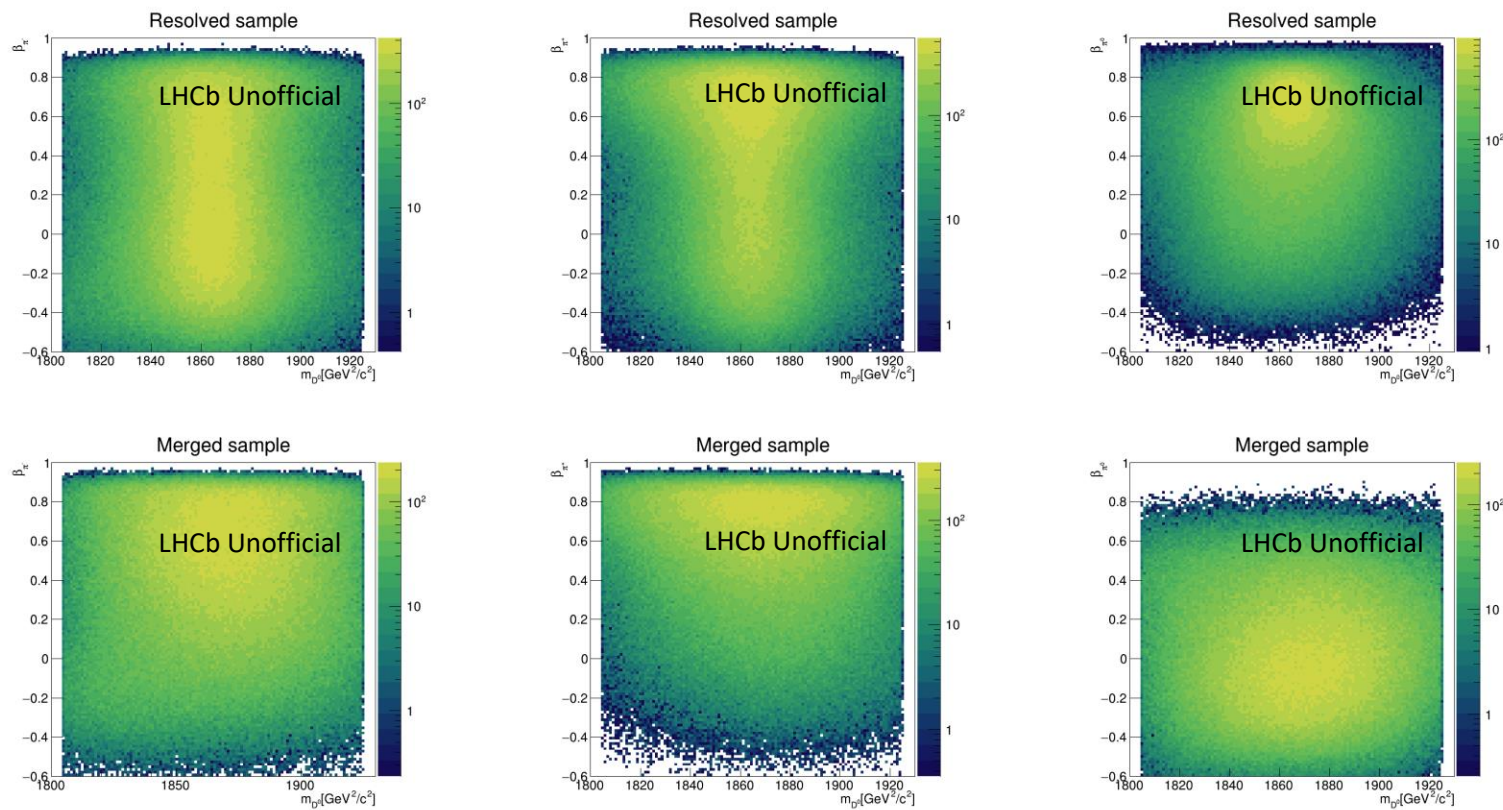
Decay Tree Fitter (DTF)

- The kinematic variables obtained by the DecayTreeFitter (DTF) algorithm, after refitting the decay chain with additional kinematic constraints, will be used in the following steps:
- The DTF simultaneously considers all of the tracks within the decay topology. It then updates all the particle kinematics based on a set of external constraints, such as the known invariant mass of their vertex, to give the best vertex fit.



Resolved, in signal region

Data Selection: mis-ID BKG

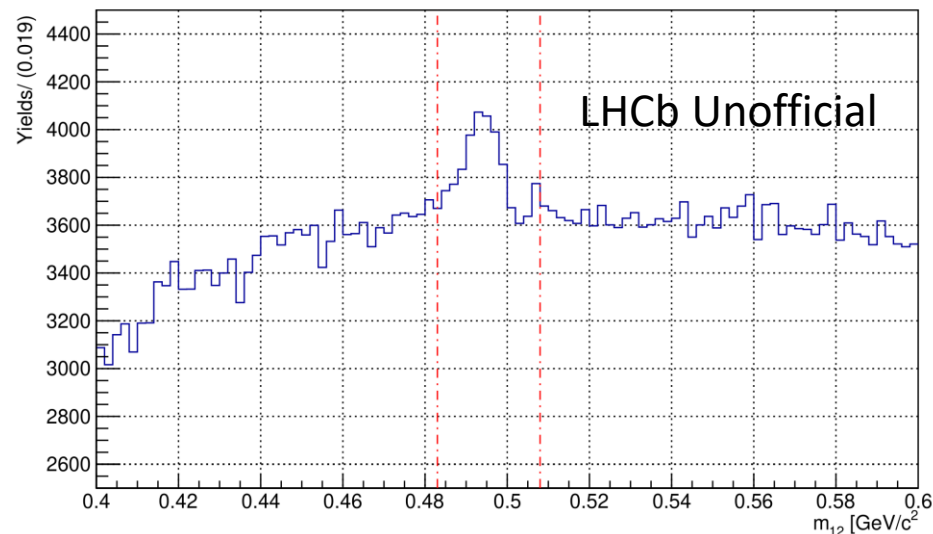
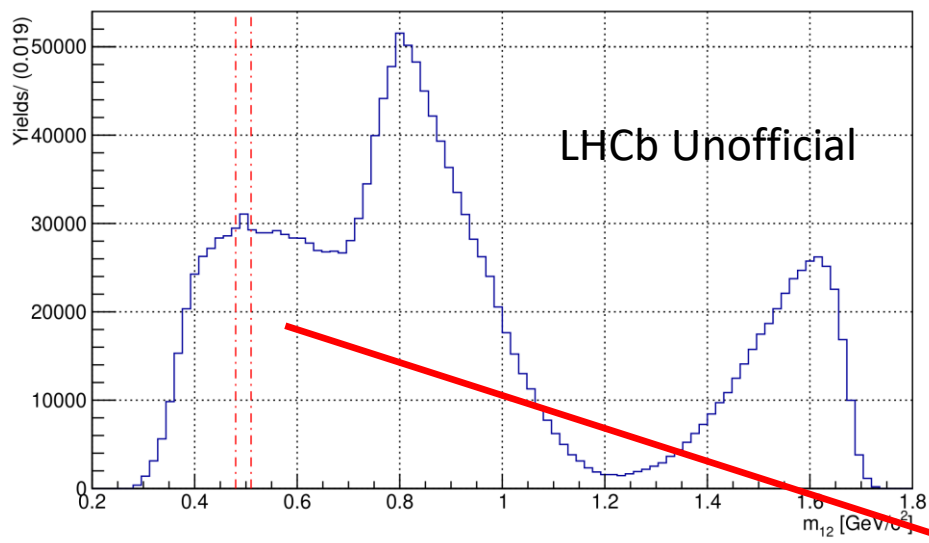


$$p_{k,asym} = \frac{|p_i| + |p_j| - |p_k|}{|p_i| + |p_j| + |p_k|}$$

- Momentum asymmetries for the three particles after all selection
- No obvious mis-ID BKG found

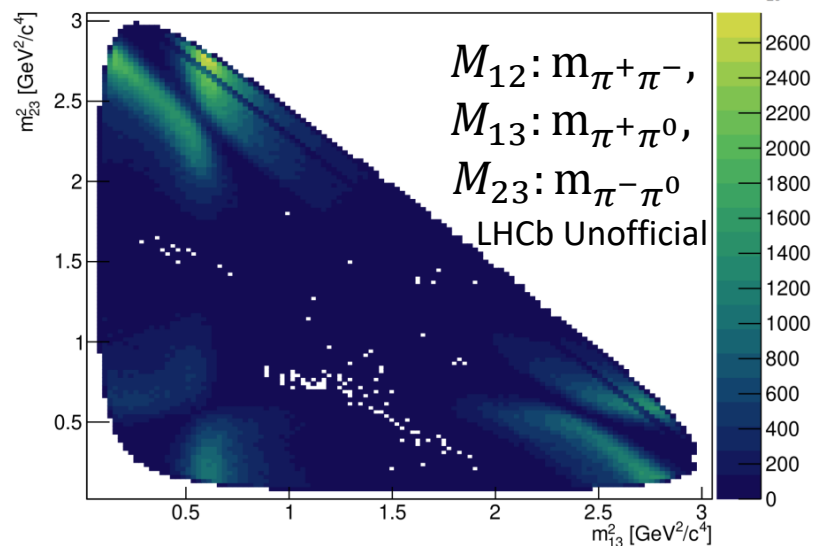
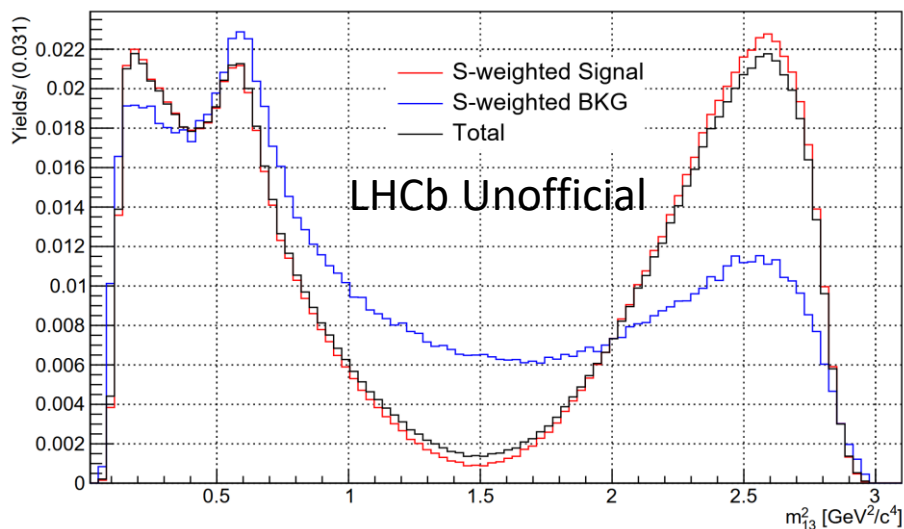
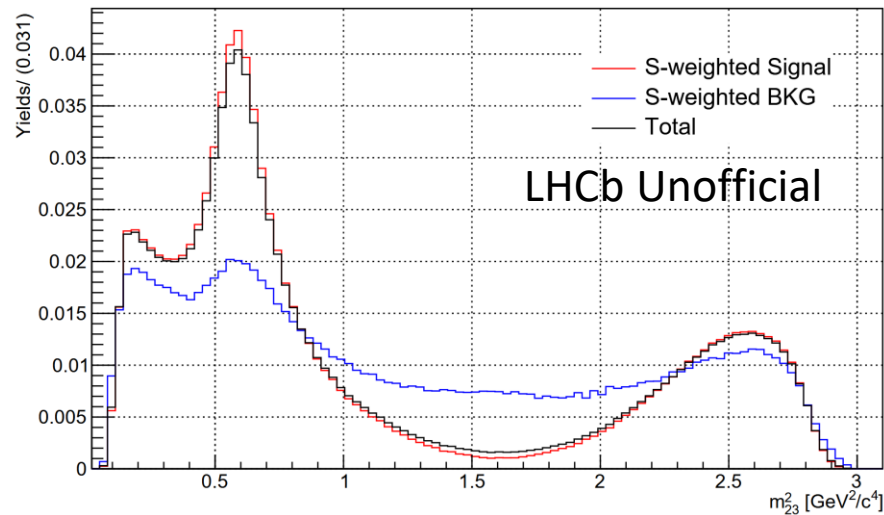
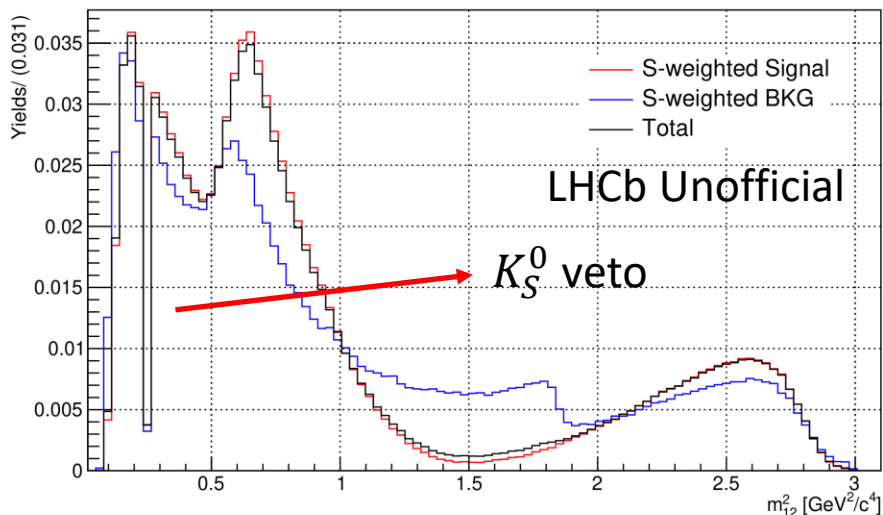
Data selection: K_S^0 mass veto

- The presence of the real K_S^0 meson in the data sample via decay $D^0 \rightarrow K_S^0 \pi^0$ is observed in our sample.
- Thus, a 15 MeV K_S^0 mass veto is applied to simply remove this decay channel.
- Signal yield decrease: $\sim 3\%$



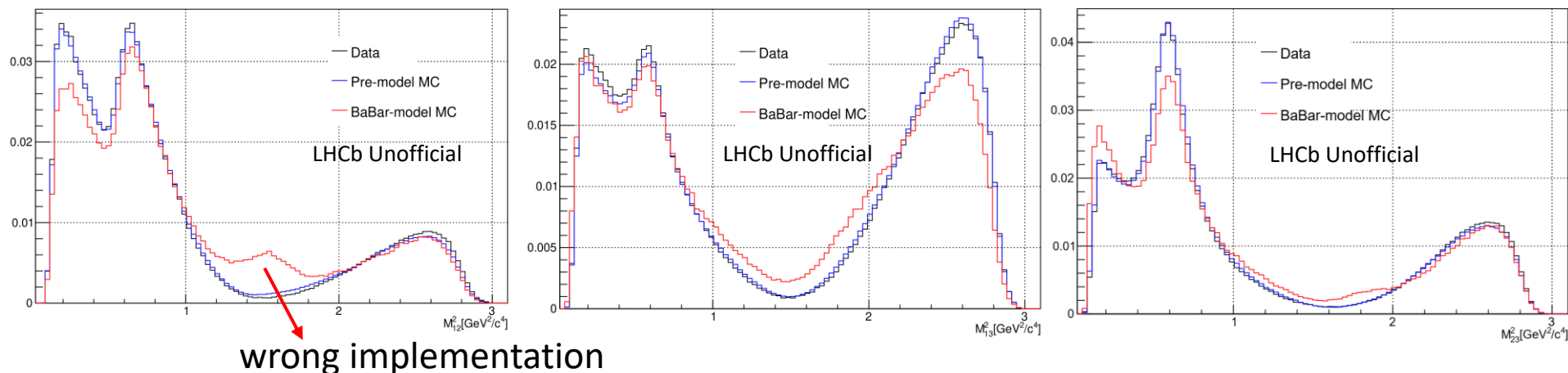
Dalitz plot

- In the following amplitude fit, the input data combines both resolved and merged sample. The background is subtracted using the sPlot technique.



Simulation sample

- The LHCb simulation sample is used:
 - Input as the signal part for the MVA classifier training
 - Input as the integration sample in the amplitude fit
- A preliminary model MC sample (3.45 M events), which looks similar to the BaBar model, is generated and passed through full selection criteria
 - Stripping + trigger + offline + MVA (resolved only)
 - MC Truth matched
- A series of corrections are also applied to improve the consistency between MC/data:
 - PID correction is applied to the PID variables $\text{PID}_K(\pi^\pm)$ using the [PIDGen2](#) tool
 - Kinematic reweighting for both MC samples using as target S-weighted signal data



Amplitude Fitting: S-wave

- S-wave possibly includes several overlapping resonances
- Approach for the S-wave description:
 - K-matrix formalism
 - 5 poles and 5 channels (details of parameters in Backup)
 - QMIPWA method (used as the nominal method)

| Resonance | $m(\text{MeV}/c^2)$ | $\Gamma(\text{MeV}/c^2)$ |
|---------------|---------------------|--------------------------|
| $f_0(980)$ | 990 ± 20 | $10 - 100$ |
| $f_0(1370)$ | $1200 - 1500$ | $200 - 500$ |
| $f_0(1500)$ | 1506 ± 6 | 112 ± 9 |
| $f_0(1710)$ | 990 ± 20 | $10 - 100$ |
| $\sigma(500)$ | $400 - 550$ | $100 - 800$ |

$$\mathcal{A}_{S\text{-wave}} = \sum_{j=1}^n [I - i\hat{K}\rho]_{ij}^{-1} \hat{P}_j$$

$$\hat{P}_j = \sum_{\alpha} \frac{\beta_{\alpha} g_{\alpha i}}{m_{\alpha}^2 - m^2} + f_i^{prod} \frac{1 - s_0^{prod}}{m^2 - s_0^{prod}}$$

$$i = \pi\pi \text{ (}\pi\pi \text{ S-wave)}$$

$$j = \pi\pi, KK, \eta\eta, 4\pi, \eta\eta' \text{ (5 poles)}$$

$$\alpha = 1, 2, 3, 4, 5 \text{ (corresponding 5 channel)}$$

Amplitude Fitting: Fit quality

- Fit quality (sWeighted):

- $$\text{FCN} = -2 \log(\mathcal{L}_P) = -2 \frac{\sum_i s w_i}{\sum_i s w_i^2} \sum_i s w_i \log(P(x; c))$$

$$= -2 \frac{\sum_i s w_i}{\sum_i s w_i^2} \sum_i s w_i [\log(|\mathcal{A}(x; c)|^2) + \log(\epsilon(x) R_3(x)) - \log(I(c))]$$

Model
independent

Only term relevant
to efficiency

- $$\chi^2 / \text{ndof}: \chi^2 = \sum_{i \in \text{bins}} \frac{(N_i - \langle N_i \rangle)^2}{\sigma_i^2 + \bar{\sigma}_i^2} \quad \sigma = \sqrt{N_i}$$
$$\text{ndof} = [N_{\text{bins}} - N_{\text{parameters}} - 1] \quad \bar{\sigma} = \text{err}_{\langle N_i \rangle}$$

Amplitude fitting: S-wave

- QMIPWA model is used for the S-wave description
- The $s(\pi^+\pi^-)$ spectrum is binned
- In each bins, the amplitude is determined by two real constants, a_k and ϕ_k :

$$\mathcal{A}_{S-Wave}^k = a_k e^{i\phi_k}$$

- A cubic spline interpolation is used to describe the S-wave amplitude at any point in $s(\pi^+\pi^-)$:

$$\mathcal{F}(x) = a_i + b_i x + c_i x^2 + d_i x^3$$

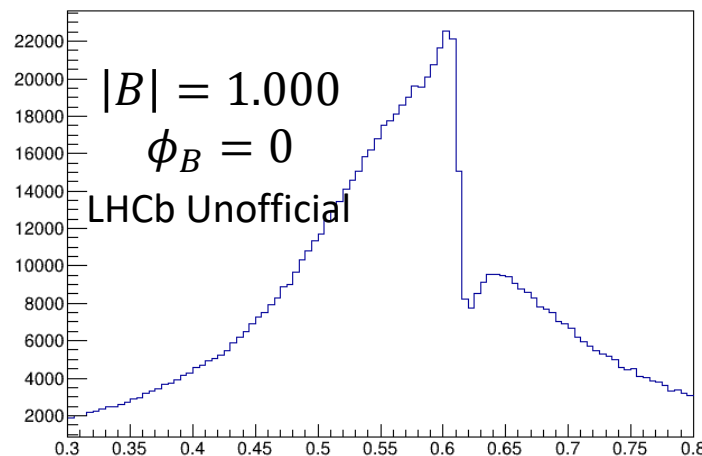
- Limitation:
 - P- and D-waves assumed to be well parametrised and included via Isobar model.
 - Need for a careful study of the binning scheme in order to improve the description in specific regions
- In our baseline model, the S-wave is constructed with the QMIPWA method using an uniform binning scheme (30 bins)

$\rho - \omega$ mixing lineshape

New $\rho - \omega$ mixing lineshape is added to the AmpGen now:

$$A_{\rho-\omega} = A_{\rho} \left[\frac{1 + A_{\omega} \Delta |B| e^{i\phi_B}}{1 - \Delta^2 A_{\rho} A_{\omega}} \right]$$

where A_{ρ} is the GS lineshape for $\rho^0(770)$ resonance, A_{ω} is the RBW lineshape for ω resonance, $\Delta = \delta(m_{\rho} + m_{\omega})$, where δ governing the electromagnetic mixing of $\rho(770)$ and $\omega(782)$, the complex value is set to be free in the amplitude fit. $|B|$ and ϕ_B are the parameters, magnitude and phase respectively, responsible for reproducing the interference pattern, which is also set to be free during the fit.



Amplitude Fitting: null test

| System | Resonance | $ \mathcal{R}(a_r) $ | $\mathcal{I}(a_r)$ | Fit Fraction [%] |
|-----------------|----------------|----------------------|----------------------------|------------------|
| | $\rho(770)^+$ | 1.0 (fixed) | 0.0 (fixed) | 74.51 ± 0.09 |
| | $\rho(770)^0$ | 0.5919 ± 0.0008 | -2.8636 ± 0.0017 | 25.96 ± 0.07 |
| | $\rho(770)^-$ | 0.6615 ± 0.0009 | -3.1309 ± 0.0026 | 32.58 ± 0.07 |
| | $\rho(1450)^+$ | 0.0907 ± 0.0013 | 2.8929 ± 0.0169 | 0.57 ± 0.02 |
| | $\rho(1450)^0$ | 0.0482 ± 0.0014 | -1.8724 ± 0.0296 | 0.16 ± 0.01 |
| | $\rho(1450)^-$ | 0.0315 ± 0.0014 | -3.1218 ± 0.0449 | 0.07 ± 0.01 |
| | $\rho(1700)^+$ | 0.1102 ± 0.0024 | 0.2507 ± 0.0209 | 0.32 ± 0.02 |
| | $\rho(1700)^0$ | 0.1403 ± 0.0025 | 2.4972 ± 0.0197 | 0.53 ± 0.03 |
| | $\rho(1700)^-$ | 0.0996 ± 0.0021 | 2.0985 ± 0.0276 | 0.26 ± 0.01 |
| | $f_2(1270)$ | 0.1147 ± 0.0007 | 0.1271 ± 0.0012 | 0.61 ± 0.01 |
| $\pi\pi$ S-wave | 30 points | | | 2.09 ± 0.01 |
| B | | 0.0297 ± 0.002 | 3.104 ± 0.0925 | |
| δ | 4.9 MeV | | | |
| | | Sum of Fit Fractions | 137.68 ± 0.16 | |
| | | χ^2/ν | $143095.26/131033 = 1.092$ | |
| | | FCN | -3045041.2 | |

From the amplitude fit result, some of the high-mass ρ resonances show low FF compared to others. The null test is used to calculate their statistical significance to the model:

$$D = -2 \ln \frac{\mathcal{L}(H_0)}{\mathcal{L}(H_i)}$$

where the $H_0(H_i)$ is the original (alternative) null hypothesis, the difference D is distributed as a χ^2 of $(N_i - N_0)$ ndof, which is converted to a significance.

- We see both resonances show a significance $>5\sigma$, which mean they are reasonable to this model.

Amplitude Fitting: Fit result (QMIPWA)

The Interferences Fit Fractions are:

| | $\rho^+(770)$ | $\rho^0(770)$ | $\rho^-(770)$ | $\rho^+(1450)$ | $\rho^0(1450)$ | $\rho^-(1450)$ | $\rho^+(1700)$ | $\rho^0(1700)$ | $\rho^-(1700)$ | $f_2(1270)$ | $\pi\pi$ S-wave |
|----------------|---------------|---------------|---------------|----------------|----------------|----------------|----------------|----------------|----------------|-------------|-----------------|
| $\rho^+(770)$ | | -7.1177 | -6.8519 | 2.3082 | -0.2466 | -0.3613 | 0.3434 | -0.1318 | 0.3756 | 0.9175 | -2.1811 |
| $\rho^0(770)$ | | | -7.0981 | -0.7243 | 0.4976 | -0.3207 | 0.1748 | 0.0001 | 0.3133 | -0.0329 | -0.2437 |
| $\rho^-(770)$ | | | | -0.2667 | -0.1711 | 0.4369 | -0.3075 | -0.1167 | -0.3286 | -0.6711 | 1.7833 |
| $\rho^+(1450)$ | | | | | -0.0653 | -0.0339 | -1.0738 | 0.0744 | 0.0346 | 0.2473 | 0.1675 |
| $\rho^0(1450)$ | | | | | | -0.0119 | 0.0164 | -0.1147 | 0.1192 | 0.0000 | 0.0000 |
| $\rho^-(1450)$ | | | | | | | 0.0000 | 0.0000 | -0.0251 | -0.0191 | 0.0724 |
| $\rho^+(1700)$ | | | | | | | | -0.0576 | 0.0000 | -0.1558 | 0.8160 |
| $\rho^0(1700)$ | | | | | | | | | 0.0000 | 0.0000 | 0.0000 |
| $\rho^-(1700)$ | | | | | | | | | | 0.0101 | -0.0604 |
| $f_2(1270)$ | | | | | | | | | | | -0.0218 |

Systematic uncertainties: overview

- Three categories of systematics:
 1. The uncertainty evaluated by comparing two different hypotheses (a & b) while fitting the same sample:
the systematic uncertainty assigned = difference on the fit parameters
 2. The uncertainty evaluated from the pseudo-experiments, where more than 1000 toy samples according to a model will be generated and fitted back to verify the input parameters:

A pull distribution is computed as:

$$\text{Pull} = \frac{|a_k^{fit}| - |a_k^{input}|}{\sigma_k^{fit}}$$

The systematic uncertainty is assigned as:

$$\sigma_k^{sys} = \sigma_k^{stat} \sqrt{\mu_k^2 + \sigma_{\mu k}^2}$$

3. The uncertainty evaluated from the external input, masses and widths of high-mass resonances from PDG. A scan of masses and widths will be performed:
The systematic uncertainty is assigned as the average of the difference between the nominal model vs. the scan result

Amplitude Fitting: Fit parameters

- Relativistic Breit–Wigner function:

$$\triangleright \hat{f}_r = \frac{1}{(m_r^2 - m_{ab}^2) - im_r \Gamma(m_{ab})}$$

- Gounaris-Sakurai function:

$$\triangleright \hat{f}_r = \frac{1 + \Gamma_0 d / m_0}{(m_0^2 - m^2) + f(m) - im_0 \Gamma(m)}$$

- The K-matrix amplitude:

$$\triangleright \hat{f}_r = P_0 = (I - i\hat{\rho}\hat{K})^{-1} \hat{P}$$

$$\hat{K}_{ab} = \left(\sum_{\alpha} \frac{g_a^{\alpha} g_b^{\alpha}}{m_{\alpha}^2 - s} + f_{ab}^{scatt} \frac{1 \text{ GeV}^2 - s_0^{scatt}}{s - s_0^{scatt}} \right) \frac{1 - s_{A_0}}{s - s_{A_0}} \left(s - s_A \frac{m_{\pi}^2}{2} \right)$$

$$\hat{P} = \frac{\sum_{\alpha} \beta^{\alpha} g_b^{\alpha}}{m_{\alpha}^2 - s} + f_{1b}^{prod} \frac{1 \text{ GeV}^2 - s_0^{prod}}{s - s_0^{prod}}$$

| m_{α} | $g_{\pi^+\pi^-}^{\alpha}$ | $g_{K\bar{K}}^{\alpha}$ | $g_{\pi\pi\pi\pi}^{\alpha}$ | $g_{\eta\eta}^{\alpha}$ | $g_{\eta\eta'}^{\alpha}$ |
|--------------|---------------------------|-------------------------|-----------------------------|-------------------------|--------------------------|
| 0.65100 | 0.22889 | -0.55377 | 0.00000 | -0.39899 | -0.34639 |
| 1.20360 | 0.94128 | 0.55095 | 0.00000 | 0.39065 | 0.31503 |
| 1.55817 | 0.36856 | 0.23888 | 0.55639 | 0.18340 | 0.18681 |
| 1.21000 | 0.33650 | 0.40907 | 0.85679 | 0.19906 | -0.00984 |
| 1.82206 | 0.18171 | -0.17558 | -0.79658 | -0.00355 | 0.22358 |
| | f_{11}^{scatt} | f_{12}^{scatt} | f_{13}^{scatt} | f_{14}^{scatt} | f_{15}^{scatt} |
| | 0.23399 | 0.15044 | -0.20545 | 0.32825 | 0.35412 |
| | | f_{21}^{scatt} | f_{31}^{scatt} | f_{41}^{scatt} | f_{51}^{scatt} |
| | | 0.15044 | -0.20545 | 0.32825 | 0.35412 |
| | | s_0^{scatt} | s_{A_0} | s_A | |
| | | -3.92637 | -0.15 | 1 | |

[EPJ A16(2003) 229]